RAA 2015 Vol. **15** No. **11**, 1823–1831 doi: 10.1088/1674–4527/15/11/005
http://www.raa-journal.org *http://www.iop.org/journals/raa*

Research in Astronomy and Astrophysics

SN 1054: A pulsar-powered supernova?

Shao-Ze Li, Yun-Wei Yu and Yan Huang

Institute of Astrophysics, Central China Normal University, Wuhan 430079, China;
lishaoze@mails.ccnu.edu.cn; yuyw@mail.ccnu.edu.cn

Received 2015 March 1; accepted 2015 May 12

Abstract The famous ancient supernova SN 1054 could have been too bright to be explained in the "standard" radioactive-powered supernova scenario. As an alternative attempt, we demonstrate that the spin-down of the newly born Crab pulsar could provide a sufficient energy supply to make SN 1054 visible at daytime for 23 days and at night for 653 days, where a one-zone semi-analytical model is employed. Our results indicate that SN 1054 could be a "normal" cousin of magnetar-powered superluminous supernovae. Therefore, SN 1054-like supernovae could be a probe to uncover the properties of newly born neutron stars, which provide initial conditions for studies on neutron star evolutions.

Key words: supernovae: individual (SN 1054) — pulsars: general — radiation mechanisms: general

1 INTRODUCTION

Supernovae are a kind of luminous explosion at the end of stellar evolution, which can transiently outshine their entire host galaxy. According to the different natures of their progenitors, the general concept of "supernovae" can be divided into three different types, i.e., due to the core collapse of a massive star, due to a super-Chandrasekhar disruption or accretion-induced collapse of a white dwarf (Canal & Schatzman 1976; Nomoto & Kondo 1991), and due to the merger of a neutron star-neutron star or neutron star-black hole binary (Li & Paczyński 1998). The bright emission of supernovae is usually powered by the decay of radioactive elements synthesized in supernova ejecta. Therefore, in view of an obviously small ejecta mass, the transients happening while a white dwarf collapses or when compact objects merge are in fact usually not classified as supernovae, but are sometimes called kilonovae. However, some recently-discovered rapidly evolving and luminous transients could overturn such a conventional understanding, because their luminosities can be significantly enhanced to be $\sim 10^{43}\ \mathrm{erg\ s^{-1}}$ by a remnant spinning-down neutron star (Yu et al. 2013, 2015).

In fact, the effect of a spinning-down neutron star on powering transient emission could widely exist. For example, a remarkable number of so-called superluminous supernova (SLSN) events have been discovered during recent years, which have bolometric luminosity about 50 times higher than those of Type Ia supernovae (Gal-Yam 2012). In the radioactive scenario for supernovae, the energy is usually supplied by the decay of ^{56}Ni to ^{56}Co and then to ^{56}Fe, but in the core-collapse case the production of ^{56}Ni is usually considered to be ineffective. In contrast, the high luminosity of SLSNe requires an extremely large amount of ^{56}Ni, e.g., $5\,M_{\odot}$ for SN 2007bi (Gal-Yam et al. 2009) and $22\,M_{\odot}$ for SN 2006gy (Smith et al. 2007). Therefore, it has been suggested that a newly born, rapidly

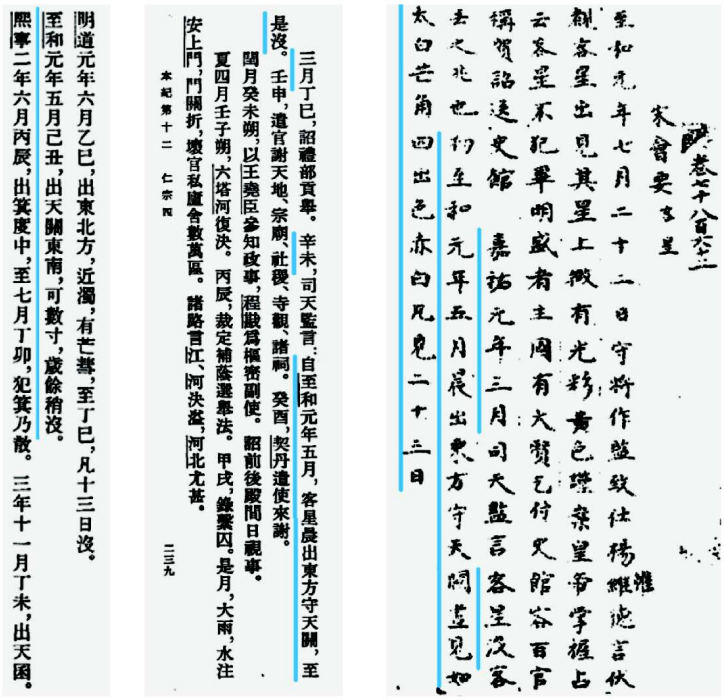

Fig. 1 The ancient records about SN 1054, marked by blue lines, in Chinese historical documents. The left and middle pictures come from *Song Shi* and the right picture comes from *Song Huiyao Jigao*.

rotating and highly-magnetized neutron star could play a substantial role in powering the SLSN emission as an alternative energy source (Woosley 2010; Kasen & Bildsten 2010). The success of this scenario has been well exhibited by some example fittings to SLSN light curves (e.g., Inserra et al. 2013; Nicholl et al. 2013). It is further indicated that each type of general supernova can be separated into two subtypes due to radioactivity and spin-down of a neutron star if a remnant neutron star exists.

SN 1054, which is famous for its remnant of the Crab Nebula (Lundmark 1921; Hubble 1928; Rudie et al. 2008), was first recorded by Chinese astronomers on 1054 July 4. Some Japanese and Arab documents in later centuries provided some independent confirmations. A summary of the historical records can be found in Green & Stephenson (2003).

As shown in Figure 1, Chinese historical documents said that SN 1054 could be seen by the naked eye during daytime for 23 days following 1054 July 4, which indicated it had an apparent visual magnitude of at least -5 mag. By considering its distance of 2.0 kpc (Trimble 1973) and the Galactic extinction of $A_{\rm v} = 1.6$ mag (Miller 1973), the absolute visual magnitude can be estimated to be $M_{\rm v} = -18.1$ mag ($\sim 6 \times 10^{42}$ erg s^{-1} in the visual band). As it faded, SN 1054 could still be visible at night until 1056 April 6, 653 days after the explosion. The limiting apparent magnitude for a night observation using the naked eye is about 5.5 mag, which corresponds to an absolute magnitude of $M_{\rm v} = -7.7$ mag ($\sim 4 \times 10^{38}$ erg s^{-1} in the visual band). Such basic features of the light curve of SN 1054 have been extensively discussed (e.g., Minkowski 1971; Chevalier 1977; Clark & Stephenson 1977; Wheeler 1978). Due to the existence of the Crab pulsar, SN 1054 can be confirmed to be a core-collapse supernova. According to properties of the Crab Nebula, the mass of

its progenitor can be estimated to be $\sim 8-10\ M_\odot$ (Nomoto et al. 1982). Some detailed calculations showed that, for such progenitor masses, the mass of ^{56}Ni produced during the supernova could be about $\sim 0.002\ M_\odot$ (Mayle & Wilson 1988). With such a small amount of ^{56}Ni, it seems impossible to explain the historical records of SN 1054 by the "standard" radioactive-powered scenario (see Appendix A for a detailed calculation). Therefore, some other energy deposits are alternatively required to generate the bright SN 1054 emission (Sollerman et al. 2001; Smith 2013), although its luminosity is normal.

Being inspired by SLSNe and considering the existence of the Crab pulsar, we propose that SN 1054 could be dominantly driven by the spin-down of the newly born Crab pulsar instead of radioactivity, as previously suggested by Sollerman et al. (2001) but who did not conduct a detailed investigation. Such an alternative scenario is obviously natural, as the pulsar is still powering the Crab Nebula today. In other words, we propose that SN 1054 could be a "normal" cousin of millisecond-magnetar-powered SLSNe.

A simple semi-analytical model is established in Section 2 to estimate the supernova light curve. In Section 3, we fit the ancient observation using this model and several groups of best fit parameters are given. Section 4 gives conclusion and discussions. The radioactive-powered scenario is also briefly discussed in Appendix A.

2 THE SUPERNOVA LIGHT CURVE MODEL

2.1 Spin-down of a Pulsar

The energy that a pulsar can provide to power a supernova mainly comes from the spin-down of the pulsar. As usual, the evolution of angular frequency Ω of the pulsar can generally be expressed in terms of power-law behavior with a braking index n, i.e.,

$$\dot{\Omega} = -K\Omega^n. \tag{1}$$

With a constant of proportionality K, the above equation gives $\Omega = \Omega_{\rm i}(1 + t/t_{\rm sd})^{-1/(n-1)}$, where the spin-down timescale reads $t_{\rm sd} = [(n-1)K\Omega_{\rm i}^{n-1}]^{-1}$ and the subscript "i" represents the initial values. Then the spin-down luminosity of a pulsar can be written as

$$L_{\rm sd} = -I\Omega\dot{\Omega} = L_{\rm sd,i}\left(1 + \frac{t}{t_{\rm sd}}\right)^{-\frac{n+1}{n-1}}, \tag{2}$$

where I is the moment of inertia of the pulsar with a typical value of $10^{45}\ {\rm g\,cm^2}$ and $L_{\rm sd,i} = IK\Omega_{\rm i}^{n+1}$. The total energy budget that can be injected into supernova ejecta should be limited by the initial rotational energy of the pulsar, given as $E_{\rm tot} = \frac{1}{2}I\Omega_{\rm i}^2 = 2\times10^{52}(P_{\rm i}/{\rm ms})^{-2}{\rm erg}$ where $P_{\rm i} = 2\pi/\Omega_{\rm i}$ is the initial spin period.

2.2 Emission of Supernova Ejecta

In view of the sparsity of historical records related to SN 1054, a one-zone semi-analytical model is adopted to simulate the supernova light curve (Arnett 1980; Kasen & Bildsten 2010). By invoking the one-zone diffusion equation, the bolometric luminosity of a supernova, L, can be expressed as (Kasen & Bildsten 2010; Kotera et al. 2013)

$$\frac{L}{4\pi R^2} = \frac{c}{3\kappa\rho}\frac{\partial E_{\rm int}/V}{\partial r} \approx \frac{c}{3\kappa\rho}\frac{E_{\rm int}/V}{R}, \tag{3}$$

where R is the radius of the supernova ejecta, κ the opacity, ρ the density, $E_{\rm int}$ the internal energy, and V the volume. For optical photons, $\kappa \sim 0.2\,{\rm cm^2\,g^{-1}}$, which is dominated by electron scattering.

The above equation is only valid for optically thick ejecta with an optical depth of $\tau = \kappa\rho R = 3\kappa M/(4\pi R^2) > 1$, where $M = \rho V$ is the total mass of the ejecta. More generally, it should be written as

$$L = \frac{E_{\rm int}c}{\tau R}, \qquad \text{for } t \le t_\tau, \tag{4}$$

$$= \frac{E_{\rm int}c}{R}, \qquad \text{for } t > t_\tau, \tag{5}$$

where t_τ represents the time for the optical thick-thin transition.

With the energy supply from the pulsar, the evolution of the internal energy of the supernova ejecta can be determined by the energy conservation law as

$$\frac{\partial E_{\rm int}}{\partial t} = \xi L_{\rm sd} - L - p\frac{\partial V}{\partial t}, \tag{6}$$

where ξ is the energy injection efficiency and the work $-pdV$ represents the energy loss due to adiabatic expansion of the ejecta with p being pressure. By taking the radiation-dominated equation of state $p = E_{\rm int}/3V$, the above equation can be rewritten as (Kasen & Bildsten 2010)

$$\frac{1}{t}\frac{\partial E_{\rm int}t}{\partial t} = \xi L_{\rm sd} - L\,. \tag{7}$$

Simultaneously, due to the adiabatic expansion, the supernova ejecta can be somewhat accelerated and then the evolution of its velocity v is determined by

$$\frac{dv}{dt} = \frac{4\pi R^2 p}{M} \tag{8}$$

with

$$\frac{dR}{dt} = v\,. \tag{9}$$

Finally, combining Equations (7), (8) and (9), we can obtain a bolometric light curve for a pulsar-powered supernova. An analytical analysis of the temporal behaviors of the light curves can be found in Yu et al. (2015).

2.3 Leakage of Hard Emission

The electromagnetic energy released from a pulsar, which could be associated with a remarkable number of electron-positron pairs, can ultimately generate a pulsar wind nebula behind the supernova ejecta. The leptons in the nebula are accelerated to a relativistic speed and mostly lose their energy by forming X-rays and gamma-rays through synchrotron and inverse-Compton radiation (Kotera et al. 2013). It should be noticed that the opacity of the supernova ejecta with respect to the X-rays and gamma-rays is very complicated and energy-dependent. Specifically, for X-rays with energy $\sim 0.1-100$ keV, the opacity is dominated by photoelectric absorption, while very hard X-rays and gamma-rays predominantly experience Compton scattering above $\sim$ 100 keV and pair production above $\sim$ 10 MeV. As a result, the opacity varies from $\sim 10^6$ cm^{2}g^{-1} for $\sim$ 100 keV to ~ 0.01 cm^{2}g^{-1} above $\sim$ 10 MeV (see fig. 8 in Kotera et al. 2013). A similar value of $\kappa_\gamma \sim 0.03$ cm^2 g^{-1} is also obtained by Colgate et al. (1980), Woosley et al. (1989) and Swartz et al. (1995) for an energy of about 2 MeV corresponding to gamma-rays from radioactive decay of ^{56}Ni and ^{56}Co. Therefore, while most energy of the pulsar wind emission is absorbed by the supernova ejecta, its highest-energy emission could first escape from the ejecta (Metzger et al. 2014). By considering such a

Table 1 Parameters for the best fittings to SN 1054

n	K (s^{n-2})	$P_{\rm i}$ (ms)	$t_{\rm sd}$ (d)	$L_{\rm sd,i}$ (erg s^{-1})	$v_{\rm f}$ (10^3 km s^{-1})
1.5	5.7×10^{-9}	6.8	1.3×10^{2}	1.5×10^{44}	2.9
2	4.6×10^{-10}	5.7	2.3	6.2×10^{44}	3.6
2.5	3.2×10^{-11}	4.5	4.7	3.2×10^{45}	4.6
3	1.7×10^{-12}	3.7	1.2	1.4×10^{46}	5.6

leakage effect, the trapping factor of the pulsar wind emission in the supernova ejecta (i.e., the energy injection efficiency ξ) can be roughly estimated by (e.g., Wang et al. 2015)

$$\xi \approx 1 - e^{-\tau_\gamma}\,, \tag{10}$$

where $\tau_\gamma = \kappa_\gamma \rho R$ is the optical depth of the supernova ejecta for gamma-rays. The above rough estimation can be valid as long as the pulsar wind emission is nearly equally allotted to X-rays and gamma-rays (> 10 MeV). Following the theoretical calculations mentioned above, we adopt $\kappa_\gamma \sim 0.01\ {\rm cm^2\ g^{-1}}$, which could also be consistent with some constraints from the fittings to the late-time light curves of some SLSNe (Wang et al. 2015; Chen et al. 2014).

3 FITTING TO THE OBSERVATION OF SN 1054

The modeled bolometric light curve cannot be directly confronted with observational records of SN 1054, because these records only include visual luminosities. Therefore, a bolometric correction (BC) to the observation is required, which, however, depends on the uncertain radiation spectrum. Some previous works suggested that the BC of supernovae is less than one magnitude during the peak, and would become several magnitudes in the late time (e.g., Bersten & Hamuy 2009, Lyman et al. 2014). Here we use a black body spectrum with an effective temperature of $T_{\rm eff} = (L/4\pi\sigma R^2)^{1/4} \sim 6000$ K to give an estimation of BC ≈ 0.5 mag for the peak luminosity, where σ is the Stefan-Boltzmann constant and the visual frequency range is taken to be $\nu = (3.8 \sim 7.9)\times10^{14}$ Hz. The temperature used here is much lower than the internal temperature in the ejecta which is described as $(E_{\rm int}/aV)^{1/4}$, where a is the radiation density constant. As shown in Equation (3), just the temperature gradient leads to the thermal flux. In late time, the spectrum could deviate from the black body and the BC could become larger because the spectral peak could shift out of the visual band. For simplicity, we take BC ≈ 2 mag for the data at day 653, according to the calculation for SN 1987A by Sollerman et al. (2001). The visual and bolometrically-corrected data are presented in Figure 2 by open and solid circles, respectively.

With the energy supply from the pulsar using different pulsar parameters, we provide some example fittings to the observation in Figure 2, where the other model parameters are taken as $M = 4.6\ M_\odot$ and $v_{\rm i} = 1000\,{\rm km\ s^{-1}}$. Obviously, with appropriate pulsar parameters, the historical observation can be well explained by the model, which indicates that SN 1054 could be a pulsar-powered supernova. Following such a consideration, some constraints on the parameters, i.e., n, K and $P_{\rm i}$ (or n, $t_{\rm sd}$ and $P_{\rm i}$), of the nascent Crab pulsar can be derived from the observation of SN 1054. For different values of n, we firstly constrain the parameters K and $P_{\rm i}$ by the luminosity during the first 23 days. The results are shown by the lines in Figure 3. Secondly, by taking into account the data at day 653, the constraints can be further fixed at some points on the lines as labeled by the solid circles in Figure 3. The parameter values of these points are listed in Table 1. As shown, the initial period of the pulsar is found to be a few milliseconds, but the spin-down timescale could vary within a wide range.

Accompanying the heating of the supernova ejecta, a remarkable fraction of the pulsar-injected energy would be transformed into kinetic energy of the ejecta. The resultant speeds at day 1000 (denoted by $v_{\rm f}$) are listed in Table 1, which are about several thousand kilometers per second. The larger

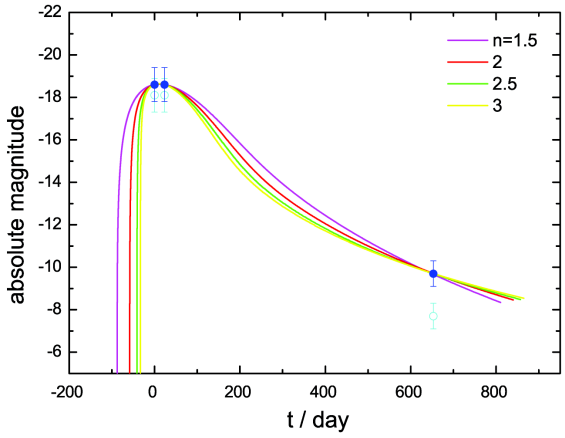

Fig. 2 Example fittings to the historical observation of SN 1054 by the pulsar-powered supernova model for different braking indices as labeled. The corresponding values of the other pulsar parameters are listed in Table 1. The solid and open circles represent the bolometrically-corrected and uncorrected observations, respectively. The error bars of the magnitude (i.e., ± 0.8 mag for day 1 and day 23 and ± 0.6 mag for day 653) are adopted from Smith (2013), which were estimated with the uncertainties in both distance and Galactic extinction.

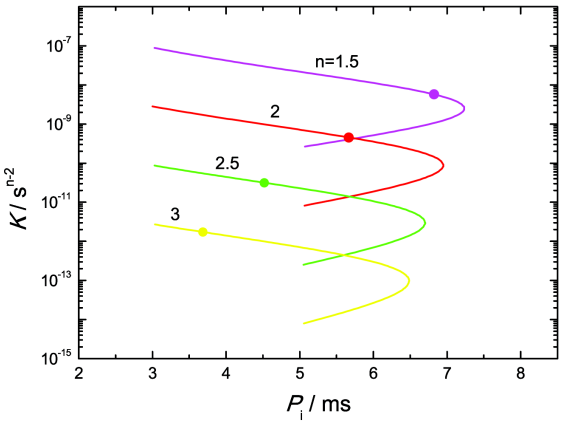

Fig. 3 The parameter space for the best fittings to the observation of SN 1054. While the lines for different n are required by the luminosity during the first 23 days, the solid circles are obtained by combining the constraints from the luminosity at day 653.

the braking index of the pulsar is, the higher the accelerated velocity is. However, present observations of the remnant Crab Nebula require SN 1054 to be "under energetic," with a kinetic energy of $\sim 10^{50}$ erg (Chevalier 1977). More specifically, the expansion velocity of the supernova ejecta should not be much higher than $1500\,\mathrm{km\ s^{-1}}$ in order to be consistent with the present size of the Crab Nebula. Therefore, a small braking index appears to be preferred. In any case, more stringent constraints on the pulsar parameters call for more observational information, which however cannot be acquired for SN 1054.

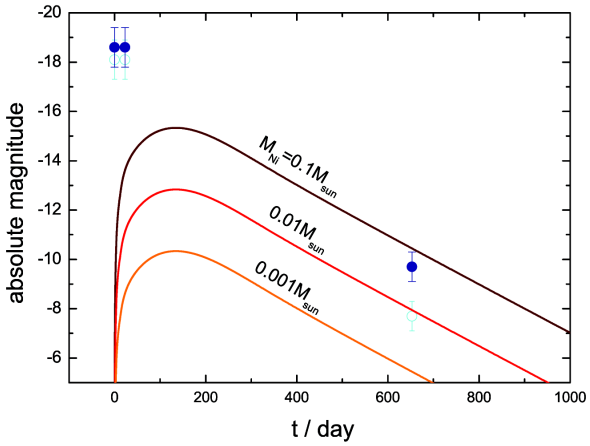

Fig. 4 A comparison between the observation of SN 1054 and some supernova light curves powered by radioactivities for different masses of ^{56}Ni.

4 CONCLUSION AND DISCUSSION

In the "standard" model, the energy deposition of supernovae is provided by the radioactive elements synthesized during the explosion. However, the basic observational features of the famous ancient case of SN 1054 cannot be explained in this scenario. Therefore, a much larger energy deposition is required to make the supernova visible at night for 653 days. In this paper we demonstrate that such an alternative energy deposition could be contributed by the spin-down of the newly born Crab pulsar. Such a pulsar energy injection model was previously proposed for gamma-ray burst afterglows (Dai & Lu 1998a,b; Yu et al. 2010) and in particular SLSNe (Woosley 2010; Kasen & Bildsten 2010), where the pulsars are usually found to be magnetars. Our work indicates that SN 1054 could be a "normal" cousin of SLSNe, although its luminosity is normal. These pulsar-powered supernovae enable us to probe the properties of newly born neutron stars, which provide peculiar initial conditions for studies on neutron star evolutions. The present braking index of the Crab pulsar is measured to be $n = 2.519 \pm 0.002$ (Lyne et al. 2015). Furthermore, according to its present period of $P(t_0) = 33$ ms and period derivative of $\dot{P}(t_0) = 4.22 \times 10^{-13}$ s s^{-1} (Lyne & Graham-Smith 2012), the present value of K can be calculated to be 4.9×10^{-15}s$^{1/2}$. The obvious difference between the initial and present values of n and K indicates a significant evolution of the braking mechanism of the pulsar occurred during the past one thousand years. Such an evolution could be caused by material accretion and outflow, gravitational radiation, and in particular the evolution of the magnetic fields that includes both the associated strength and structure.

Finally, instead of the pulsar power, the kinetic energy of the SN ejecta could also provide an energy source for radiation from the supernova, if dense circum-stellar material can be produced by the stellar wind before the collapse. In that case, the kinetic energy of the ejecta (i.e. the remaining envelope) can be converted into internal energy by the shock, which could effectively raise the peak luminosity in the early times (Smith et al. 2008; Smith 2013).

Acknowledgements This work is supported by the National Natural Science Foundation of China (Grant No. 11473008), the funding for the Authors of National Excellent Doctoral Dissertations of China (Grant No. 201225), and the Program for New Century Excellent Talents in University (Grant No. NCET-13-0822).

Appendix A: RADIOACTIVE-POWERED SUPERNOVAE

As a standard consideration, here we present the supernova light curves powered by the decay of nuclei, specifically, the dominant process of ^{56}Ni$\rightarrow^{56}$Co$\rightarrow^{56}$Fe. The numbers of nuclei N_i in a decay chain are determined by the Bateman equations:

$$\frac{dN_{\rm Ni}}{dt} = -\frac{N_{\rm Ni}}{\tau_{\rm Ni}}, \tag{A.1}$$

$$\frac{dN_{\rm Co}}{dt} = \frac{N_{\rm Ni}}{\tau_{\rm Ni}} - \frac{N_{\rm Co}}{\tau_{\rm Co}}, \tag{A.2}$$

where $\tau_{\rm Ni} = 8.8$ day and $\tau_{\rm Co} = 111.3$ day are the mean lifetimes of the nuclei. The energy released during these processes is carried by the produced gamma-rays and positrons, where the latter one is relatively subordinate. The gamma-ray energy is $q_{\rm Ni}$ =1.78 MeV and $q_{\rm Co}$ =3.505 MeV for the decay per ^{56}Ni and per ^{56}Co, respectively. Then, the powers due to the decay of ^{56}Ni and ^{56}Co can be solved to give

$$\begin{aligned} L_{\rm Ni} &= \frac{q_{\rm Ni} N_{\rm Ni}(0)}{\tau_{\rm Ni}} \exp\left(-\frac{t}{\tau_{\rm Ni}}\right) \\ &= 8.0\times10^{43}\left(\frac{M_{\rm Ni}}{M_\odot}\right) f_\gamma \exp\left(-\frac{t}{\tau_{\rm Ni}}\right)\ {\rm erg\ s^{-1}}, \end{aligned} \tag{A.3}$$

and

$$\begin{aligned} L_{\rm Co} &\approx \frac{q_{\rm Co} N_{\rm Ni}(0)}{\tau_{\rm Co}} \frac{\tau_{\rm Co}}{\tau_{\rm Co}-\tau_{\rm Ni}} \exp\left(-\frac{t}{\tau_{\rm Co}}\right) \\ &= 1.4\times10^{43}\left(\frac{M_{\rm Ni}}{M_\odot}\right) f_\gamma \exp\left(-\frac{t}{\tau_{\rm Co}}\right)\ {\rm erg\ s^{-1}}, \end{aligned} \tag{A.4}$$

where $M_{\rm Ni}$ is the initial total mass of ^{56}Ni and f_γ represents the fraction of gamma-rays trapped in the ejecta. For simplicity, we assume $f_\gamma = 1$, which actually could become much smaller with a decrease in the optical depth. By substituting Equations (A.3) and (A.4) into Equation (7), we plot some radioactive-powered supernova light curves in Figure 4 with varying values of $M_{\rm Ni}$ as labeled. Although some uncertainties still exist in the time zero-point of the light curves, Figure 4 confirms that the luminosity of SN 1054 during the first 23 days cannot be accounted for with only radioactive power. Of course, one may suggest that a much higher and much narrower peak could be produced by some other mechanisms (e.g., the recombination wave), which, however, could not influence the late emission. Therefore, as pointed out by Sollerman et al. (2001), the radioactive-dominated scenario can be basically ruled out by the last observational record at day 653, because the required mass of ^{56}Ni is much higher than what an $8-10\ M_\odot$ progenitor can provide. Then, a much larger alternative energy deposition is undoubtedly demanded for both early and late emission of SN 1054.

References

Arnett, W. D. 1980, ApJ, 237, 541
Bersten, M. C., & Hamuy, M. 2009, ApJ, 701, 200
Canal, R., & Schatzman, E. 1976, A&A, 46, 229
Chen, T.-W., Smartt, S. J., Jerkstrand, A., et al. 2014, arXiv:1409.7728
Chevalier, R. A. 1977, in Astrophysics and Space Science Library, 66, Supernovae, ed. D. N. Schramm, 53
Clark, D. H., & Stephenson, F. R. 1977, The Historical Supernovae (Oxford [Eng.]; New York: Pergamon Press)

Colgate, S. A., Petschek, A. G., & Kriese, J. T. 1980, ApJ, 237, L81
Dai, Z. G., & Lu, T. 1998a, A&A, 333, L87
Dai, Z. G., & Lu, T. 1998b, Physical Review Letters, 81, 4301
Gal-Yam, A., Mazzali, P., Ofek, E. O., et al. 2009, Nature, 462, 624
Gal-Yam, A. 2012, Science, 337, 927
Green, D. A., & Stephenson, F. R. 2003, in Lecture Notes in Physics, 598, Supernovae and Gamma-Ray Bursters, ed. K. Weiler, 7 (Berlin: Springer Verlag)
Hubble, E. P. 1928, Leaflet of the Astronomical Society of the Pacific, 1, 55
Inserra, C., Smartt, S. J., Jerkstrand, A., et al. 2013, ApJ, 770, 128
Kasen, D., & Bildsten, L. 2010, ApJ, 717, 245
Kotera, K., Phinney, E. S., & Olinto, A. V. 2013, MNRAS, 432, 3228
Li, L.-X., & Paczyński, B. 1998, ApJ, 507, L59
Lundmark, K. 1921, PASP, 33, 225
Lyman, J. D., Bersier, D., & James, P. A. 2014, MNRAS, 437, 3848
Lyne, A., & Graham-Smith, F. 2012, Pulsar Astronomy (Cambridge: Cambridge Univ. Press)
Lyne, A. G., Jordan, C. A., Graham-Smith, F., et al. 2015, MNRAS, 446, 857
Mayle, R., & Wilson, J. R. 1988, ApJ, 334, 909
Metzger, B. D., Vurm, I., Hascoët, R., & Beloborodov, A. M. 2014, MNRAS, 437, 703
Miller, J. S. 1973, ApJ, 180, L83
Minkowski, R. 1971, in IAU Symposium, 46, The Crab Nebula, ed. R. D. Davies & F. Graham-Smith, 241
Nicholl, M., Smartt, S. J., Jerkstrand, A., et al. 2013, Nature, 502, 346
Nomoto, K., Sugimoto, D., Sparks, W. M., et al. 1982, Nature, 299, 803
Nomoto, K., & Kondo, Y. 1991, ApJ, 367, L19
Rudie, G. C., Fesen, R. A., & Yamada, T. 2008, MNRAS, 384, 1200
Smith, N., Li, W., Foley, R. J., et al. 2007, ApJ, 666, 1116
Smith, N., Chornock, R., Li, W., et al. 2008, ApJ, 686, 467
Smith, N. 2013, MNRAS, 434, 102
Sollerman, J., Kozma, C., & Lundqvist, P. 2001, A&A, 366, 197
Swartz, D. A., Sutherland, P. G., & Harkness, R. P. 1995, ApJ, 446, 766
Trimble, V. 1973, PASP, 85, 579
Wang, S. Q., Wang, L. J., Dai, Z. G., & Wu, X. F. 2015, ApJ, 799, 107
Wheeler, J. C. 1978, ApJ, 225, 212
Woosley, S. E., Hartmann, D., & Pinto, P. A. 1989, ApJ, 346, 395
Woosley, S. E. 2010, ApJ, 719, L204
Yu, Y.-W., Cheng, K. S., & Cao, X.-F. 2010, ApJ, 715, 477
Yu, Y.-W., Zhang, B., & Gao, H. 2013, ApJ, 776, L40
Yu, Y.-W., Li, S.-Z., & Dai, Z.-G. 2015, ApJ, 806, L6